# IMPACT: Importance-Aware Activation Space Reconstruction

Md Mokarram Chowdhury\*

Daniel Agyei Asante

**Ernie Chang** 

Yang Li\*†

# **Abstract**

Large language models (LLMs) achieve strong performance across many domains but are difficult to deploy in resource-constrained settings due to their size. Lowrank weight matrix compression is a popular strategy for reducing model size, typically by minimizing weight reconstruction error under the assumption that weights are low-rank. However, this assumption often does not hold in LLMs. Instead, LLM activations exhibit stronger low-rank structure—prompting a shift toward minimizing activation reconstruction error.

We show that this shift alone is insufficient: activation dimensions contribute unequally to model performance, and uniform reconstruction can harm performance. We propose IMPACT, a principled framework for importance-aware activation reconstruction that links model compression decisions to their impact on model behavior. IMPACT formulates an optimization problem that considers both activation structure and gradient sensitivity, and derives a closed-form solution where the optimal reconstruction bases are the eigenvectors of an importance-weighted activation covariance matrix. This enables low-rank approximations explicitly optimized to preserve accuracy. Experiments across diverse models and tasks show that IMPACT achieves up to 48.6% greater model size reduction with accuracy comparable to state-of-the-art baselines.

# 1 Introduction

Large language models (LLMs) have achieved remarkable success across a wide range of domains. However, their massive size poses a significant barrier to deployment, particularly in resource-constrained environments. Larger models require more memory, incur slower token throughput, and demand greater computational resources during inference. As a result, there is growing urgency to develop compression techniques that can reduce model size while preserving performance.

Low-rank weight matrix compression has emerged as a widely used strategy for model compression [Xue et al., 2013, Acharya et al., 2019, Noach and Goldberg, 2020, Huang et al., 2021, Lv et al., 2023, Sharma et al., 2024]. It

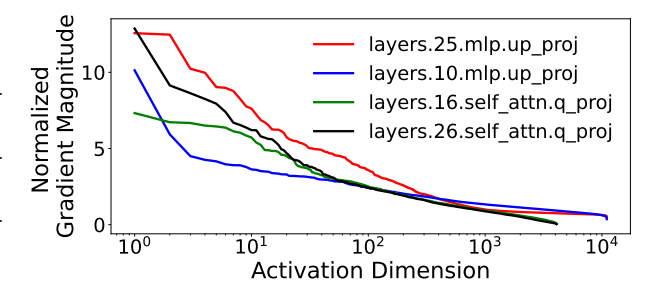


Figure 1: Normalized average gradient magnitudes across activation dimensions in Llama 2-7B on a mathematical reasoning task. Within each layer, dimensions are sorted in descending order of gradient magnitude, and each value is normalized by the mean across all dimensions. The gradient magnitudes vary substantially across activation dimensions—a pattern also consistently observed in other models and tasks.

approximates a weight matrix  $\mathbf{W} \in \mathbb{R}^{m \times n}$  as the product of two smaller matrices,  $\mathbf{W_1} \in \mathbb{R}^{m \times k}$  and  $\mathbf{W_2} \in \mathbb{R}^{k \times n}$ where  $k \ll m, n$ , thereby reducing the number of parameters. Classical methods select W<sub>1</sub> and W<sub>2</sub> to minimize the reconstruction error  $\|\mathbf{W} - \mathbf{W_1} \mathbf{W_2}\|$ , implicitly assuming that the weight matrix itself is low-rank. However, recent evidence from Yu and Wu [2023] reveals that the weight matrices in large-scale models are often not low-rank, limiting the efficacy of direct weight approximation. Interestingly, they observe that the activations—the outputs of linear layers—tend to exhibit much stronger low-rank structure. This has led to a shift in focus: instead of minimizing weight reconstruction error, some recent methods Yu and Wu [2023], Chen et al. [2021b] minimize the error in reconstructing the activations induced by those weights, achieving better empirical performance.

However, minimizing activation reconstruction error alone is insufficient to guarantee strong model performance. As shown in Figure 1, different activation dimensions vary widely in their influence on the loss: dimensions associated with large gradients are highly sensitive to reconstruction errors, whereas others contribute little even when poorly reconstructed. Thus, treating all dimensions equally during

<sup>\*</sup>Equal contribution.

<sup>&</sup>lt;sup>†</sup>Corresponding author. Email: jerryyangli@gmail.com.

 $<sup>^{1}</sup>$ The rank of a matrix is the number of linearly independent rows or columns. A low-rank matrix allows for a small k with minimal reconstruction error.

compression can disproportionately harm those that matter most—leading to greater performance degradation despite low reconstruction error. This raises a critical question:

How can we align activation reconstruction decisions with their actual performance impact?

Answering this question requires a principled framework that explicitly connects weight compression, activation reconstruction, and their contribution to the model performance—a connection that has not yet been systematically explored in the context of low-rank weight matrix compression.

To this end, we propose IMPACT, a theoretical framework that guides importance-aware activation space reconstruction. IMPACT rigorously analyzes the relationship among weight compression, activation reconstruction, and model performance. By explicitly linking reconstruction decisions to their performance impact, it provides principled guidance for selecting weights to minimize performance degradation. The framework is grounded in a formal optimization formulation, which is transformed into a more tractable domain and solved through a rigorous analytical derivation using techniques such as the Lagrange multiplier method. Despite the complexity of the derivation, the final result is remarkably simple: the optimal activation reconstruction bases are the eigenvectors of an importance-weighted activation covariance matrix  $\mathbf{C} = \operatorname{Cov}(\mathbf{y}) \odot \mathbf{M}$ , where  $\operatorname{Cov}(\mathbf{y})$  is the covariance matrix of the activations, and M is the gradient-informed importance matrix (Equations (10)–(12)). These eigenvectors yield the weight matrices  $W_1$  and  $W_2$  that minimize performance loss. We apply IMPACT to compress a variety of models across diverse datasets and show that it achieves up to 48.6% greater size reduction while maintaining performance comparable to state-of-the-art baselines.

This paper makes the following contributions:

- We introduce IMPACT, a principled theoretical framework that formally characterizes the relationship between activation reconstruction and its effect on model performance. To our knowledge, this is the first framework within the scope of low-rank weight matrix compression that directly links activation reconstruction choices to model performance.
- We derive a closed-form solution for selecting optimal reconstruction bases using an importance-weighted activation covariance matrix, enabling importanceaware low-rank compression that prioritizes activation dimensions critical to loss minimization.
- We empirically validate IMPACT across a wide range of models and tasks, showing it achieves significantly higher compression rates while maintaining performance comparable to state-of-the-art methods.

# 2 Related Work

Singular Value Decomposition (SVD) [Golub and Loan, 1983] is a widely used technique for neural network compression, offering low-rank approximations that reduce model size and improve efficiency. Prior work has applied SVD to various network components—convolutional layers, recurrent units, and embeddings—across domains such as language, speech, and vision [Xue et al., 2013, Jaderberg et al., 2014, Denton et al., 2014, Tai et al., 2016, Kim et al., 2016, Lu et al., 2016, Wen et al., 2017, Chen et al., 2018, Acharya et al., 2019, Wang et al., 2021]. More recent efforts extend these techniques to Transformer-based models [Noach and Goldberg, 2020, Huang et al., 2021, Li et al., 2023, Lv et al., 2023, Sharma et al., 2024], compressing attention and feedforward layers to enhance memory and compute efficiency.

Traditional SVD-based methods minimize weight reconstruction error by retaining top singular components, but this can discard performance-critical information. To address this, FWSVD [Hsu et al., 2022] introduces a weighted factorization scheme guided by Fisher information, assigning higher importance to influential weights.

Recent work has proposed weight compression methods that depart from minimizing weight reconstruction error and instead aim to minimize the reconstruction error of layer activations [Yu and Wu, 2023, Yuan et al., 2023, Chen et al., 2021b]. Among them, AFM [Yu and Wu, 2023] explicitly leverages the empirical observation that activations often exhibit stronger low-rank structure than weights, and optimizes the factorized weights to preserve activations. While these approaches have shown improved empirical results, they typically treat all activation dimensions equally, without fully accounting for their varying contribution to model performance.

In contrast, our work focuses on minimizing the impact of activation reconstruction on model performance. Rather than uniformly reducing reconstruction error, we prioritize preserving the most prediction-critical components of the activation. To our knowledge, this is the first framework in the context of low-rank weight matrix compression that explicitly links activation reconstruction choices to their effect on model accuracy.

# 3 The IMPACT Framework

In this section, we present IMPACT, our activation reconstruction-based model compression framework. IM-PACT identifies a set of directions that enable importance-aware activation reconstruction, minimizing compression-induced performance degradation. We first formulate the optimization problem and define the compression directions in Section 3.1, laying the foundation for performance-

preserving reconstruction. Sections 3.2 to 3.6 develop a systematic solution by transforming the activation space, deriving optimal directions via constrained optimization, and constructing the compressed model. Section 3.7 provides a complete algorithm and implementation details of the IMPACT framework.

# 3.1 Defining the Objective Function

Let  $\mathbf{y} \in \mathbb{R}^d$  be the activation produced by a specific layer of the model for a single input sample. We aim to identify a set of r orthonormal vectors  $\{\mathbf{u_1},\ldots,\mathbf{u_r}\}$  that define the directions used to reconstruct activations. Each vector satisfies  $\|\mathbf{u_k}\| = 1$  and  $\mathbf{u_i} \perp \mathbf{u_j}$  for  $i \neq j$ , with indices  $i, j, k \in \{1, \ldots, r\}$ . The reconstructed activation is denoted by  $\hat{\mathbf{y}}$ .

Our objective is to select  $\{u_k\}$  such that the reconstructed activation  $\hat{y}$  closely approximates the original activation y while preserving model performance. To this end, we define the following objective function:

$$\min f(\{\mathbf{u}_{\mathbf{k}}\}) = \alpha \mathbb{E}[\|\mathbf{y} - \hat{\mathbf{y}}\|^2] + \beta \mathbb{E}[(\ell(\mathbf{y}) - \ell(\hat{\mathbf{y}}))^2] \quad (1)$$

This objective comprises two terms:

- $\alpha \mathbb{E}[\|\mathbf{y} \hat{\mathbf{y}}\|^2]$  encourages  $\hat{\mathbf{y}}$  to be numerically close to  $\mathbf{y}$ .
- $\beta \mathbb{E}\left[(\ell(\mathbf{y}) \ell(\hat{\mathbf{y}}))^2\right]$  penalizes changes in the loss function  $\ell$  due to discrepancies between  $\mathbf{y}$  and  $\hat{\mathbf{y}}$ .

# 3.2 Bounding the Objective

We now derive an upper bound on the original objective function, providing a more tractable alternative for optimization.

**Theorem 1** (Bounding Theorem). Suppose the loss function  $\ell$  is  $C^1$ -smooth, and the activation dimension is d. Then the objective function in Equation (1) is upper bounded by:

$$f(\{\mathbf{u_k}\}) \leq \mathbb{E}\left[\left\|\sqrt{\beta d \mathbb{E}\left[\left(\frac{\partial \ell}{\partial \mathbf{y}}\right)^2\right]^\top + \alpha} \odot (\mathbf{y} - \hat{\mathbf{y}})\right\|^2\right]$$

The proof is presented in Appendix A.2. To simplify the expression and balance the two components of the objective, we set the parameters as:

$$\alpha = \eta, \quad \beta = \frac{1 - \eta}{\mathbb{E}\left[\|\frac{\partial \ell}{\partial \mathbf{y}}\|^2\right]}$$

Substituting these values into the upper bound yields:

$$h(\{\mathbf{u_k}\}) = \mathbb{E}\left[\left\|\sqrt{\frac{(1-\eta)}{\frac{1}{d}\mathbb{E}\left[\left\|\frac{\partial \ell}{\partial \mathbf{y}}\right\|^2\right]}\mathbb{E}\left[\left(\frac{\partial \ell}{\partial \mathbf{y}}\right)^2\right]^\top + \eta} \odot (\mathbf{y} - \hat{\mathbf{y}})\right\|^2\right]$$

Here,  $\odot$  denotes the Hadamard (elementwise) product. This gives the inequality:

$$f(\{\mathbf{u_k}\}) \leq h(\{\mathbf{u_k}\})$$

Directly minimizing  $f(\{\mathbf{u_k}\})$  under the orthonormal constraints

$$\|\mathbf{u_k}\| = 1$$
,  $\mathbf{u_i} \perp \mathbf{u_j}$  for  $i \neq j$ ,  $i, j, k = 1, \dots, r$ 

is analytically challenging and computationally costly. Instead, we minimize the upper bound  $h(\{\mathbf{u_k}\})$  under the same constraints, yielding an optimization problem that is tractable and efficient.

# 3.3 Activation Space Transformation

To optimize the objective  $h(\{\mathbf{u_k}\})$  under the orthonormal constraints, we transform the activations into a new space where the optimization problem can be solved analytically. Specifically, we define a transformation coefficient  $\mathbf{a}$  as:

$$\mathbf{a} = \sqrt{(1 - \eta) \frac{\mathbb{E}\left[\left(\frac{\partial \ell}{\partial \mathbf{y}}\right)^{2}\right]^{\top}}{\frac{1}{d}\mathbb{E}\left[\left\|\frac{\partial \ell}{\partial \mathbf{y}}\right\|^{2}\right]} + \eta}$$
(4)

Without loss of generality, we assume that the meanremoved reconstructed activations are given by projecting the original activations (after transformation) onto the subspace spanned by  $\{\mathbf{u_k}\}$ . Formally, we impose:

$$\mathbf{a} \odot (\hat{\mathbf{y}} - \mathbb{E}[\mathbf{y}]) = \left(\sum_{k} \mathbf{u_k} \mathbf{u_k}^{\top}\right) \mathbf{a} \odot (\mathbf{y} - \mathbb{E}[\mathbf{y}])$$
 (5)

Defining the transformed activation as

$$\tilde{\mathbf{y}} = \mathbf{a} \odot (\mathbf{y} - \mathbb{E}[\mathbf{y}])$$

we can rewrite the objective  $h(\{\mathbf{u}_k\})$  in a form that depends only on the transformed activation, as stated in the following theorem.

**Theorem 2** (Activation Space Transformation Theorem). Given the transformation  $\tilde{\mathbf{y}} = \mathbf{a} \odot (\mathbf{y} - \mathbb{E}[\mathbf{y}])$ , the objective  $h(\{\mathbf{u_k}\})$  becomes:

$$h(\{\mathbf{u_k}\}) = \mathbb{E}\left[\tilde{\mathbf{y}}^\top \left(\mathbf{I} - \sum_k \mathbf{u_k} \mathbf{u_k}^\top\right) \tilde{\mathbf{y}}\right]$$

The proof is provided in Appendix A.3.

# 3.4 Lagrange Formulation and Derivation

To solve the constrained optimization problem, we apply the method of Lagrange multipliers. Our goal is to minimize the objective  $h(\{\mathbf{u_k}\})$  subject to the normalization constraint  $\|\mathbf{u_k}\|=1$ , along with the orthogonality constraints. To enforce this, we define the Lagrangian function:

$$L(\{\mathbf{u_k}\}) = h(\{\mathbf{u_k}\}) + \sum_{k=1}^{r} \lambda_k \left(\mathbf{u_k}^{\top} \mathbf{u_k} - 1\right)$$
 (6)

where  $\lambda_k$  is the Lagrange multiplier associated with the constraint  $\mathbf{u_k}^{\top}\mathbf{u_k} = 1$ .

We derive the optimality conditions by taking the derivative of  $L(\{\mathbf{u_k}\})$  with respect to each  $\mathbf{u_k}$  and setting it to zero. Using standard results from matrix calculus, we obtain:

$$\frac{\partial L}{\partial \mathbf{u_k}} = -2\mathbf{u_k}^{\mathsf{T}} \mathbb{E} \left[ \tilde{\mathbf{y}} \tilde{\mathbf{y}}^{\mathsf{T}} \right] + \lambda_k \mathbf{u_k}^{\mathsf{T}} \tag{7}$$

To simplify notation, we define the **importance-weighted** activation covariance matrix:

$$\mathbf{C} = \mathbb{E}\left[\tilde{\mathbf{y}}\tilde{\mathbf{y}}^{\top}\right] \tag{8}$$

Substituting into Equation (7), the optimality condition becomes:

$$-2\mathbf{u_k}^{\mathsf{T}}\mathbf{C} + \lambda_k \mathbf{u_k}^T = 0 \tag{9}$$

The following theorem characterizes the structure of C.

**Theorem 3** (Importance-Weighted Activation Covariance Matrix). The matrix  $\mathbf{C}$  is equal to the Hadamard product of the activation covariance matrix  $Cov(\mathbf{y})$  and the gradient-informed importance matrix  $\mathbf{M}$ , i.e.,

$$\mathbf{C} = \operatorname{Cov}(\mathbf{y}) \odot \mathbf{M} \tag{10}$$

where

$$Cov(\mathbf{y}) = \mathbb{E}\left[ (\mathbf{y} - \mathbb{E}[\mathbf{y}])(\mathbf{y} - \mathbb{E}[\mathbf{y}])^T \right]$$
 (11)

$$\mathbf{M} = \mathbf{a}\mathbf{a}^{\top} \tag{12}$$

A detailed derivation is provided in Appendix A.4.

Remark 1. Since both Cov(y) and M are positive semidefinite, their Hadamard product C is also positive semidefinite by the Schur product theorem Zhang [2006].

Remark 2. Because Cov(y) and M are symmetric, C is symmetric as well.

# 3.5 Reconstruction Direction

From Equation (9) and the fact that C is real and symmetric, we have:

$$\mathbf{C}\mathbf{u}_{\mathbf{k}} = \lambda_k \mathbf{u}_{\mathbf{k}} \tag{13}$$

This implies that each reconstruction direction  $\mathbf{u_k}$  is an eigenvector of  $\mathbf{C}$ . We formalize this result in the following theorem:

**Theorem 4** (Reconstruction Direction Theorem). *To minimize the objective*  $h(\{\mathbf{u}_k\})$  *under the orthonormality constraints, the optimal*  $k^{\mathrm{th}}$  *reconstruction direction*  $\mathbf{u}_k$  *is the eigenvector corresponding to the*  $k^{\mathrm{th}}$  *largest eigenvalue of the importance-weighted activation covariance matrix*  $\mathbf{C}$ .

A full derivation is provided in Appendix A.5.

The reconstruction directions  $\{\mathbf{u_k}\}_{k=1}^r$  are obtained by selecting and normalizing the top r eigenvectors of  $\mathbf{C}$ . These eigenvectors are guaranteed to be orthogonal.

## 3.6 Compressed Model Representation

After obtaining the reconstruction directions  $\{\mathbf{u_k}\}_{k=1}^r$ , we construct the compressed model accordingly.

Given the relationship between the original activation y and the reconstructed activation  $\hat{y}$ :

$$\mathbf{a}\odot(\mathbf{\hat{y}}-\mathbb{E}[\mathbf{y}]) = \left(\sum_k \mathbf{u_k} \mathbf{u_k}^{ op}
ight) \mathbf{a}\odot(\mathbf{y}-\mathbb{E}[\mathbf{y}])$$

and the fact that y = Wx + b, where W and b are the original layer's weight matrix and bias, we can express the reconstructed activation  $\hat{y}$  as follows:

**Theorem 5** (Activation Reconstruction Theorem). *The* reconstructed activation  $\hat{\mathbf{y}}$ , which satisfies the projection condition

$$\mathbf{a}\odot(\mathbf{\hat{y}}-\mathbb{E}[\mathbf{y}]) = \left(\sum_k \mathbf{u_k} \mathbf{u_k}^{ op}
ight) \mathbf{a}\odot(\mathbf{y}-\mathbb{E}[\mathbf{y}])$$

is given by:

$$\begin{split} \mathbf{\hat{y}} &= \left[\mathbf{U} \oslash (\mathbf{a} \cdot \mathbf{1_r}^\top)\right] \left[ (\mathbf{U} \odot (\mathbf{a} \cdot \mathbf{1_r}^\top))^\top \mathbf{W} \right] \mathbf{x} \\ &+ (\mathbf{U} \oslash (\mathbf{a} \cdot \mathbf{1_r}^\top)) (\mathbf{U} \odot (\mathbf{a} \cdot \mathbf{1_r}^\top))^\top (\mathbf{b} - \mathbb{E}[\mathbf{y}]) + \mathbb{E}[\mathbf{y}] \end{split}$$

where  $\mathbf{U} = [\mathbf{u}_1, \dots, \mathbf{u}_r]$ ,  $\mathbf{1_r}$  is an r-dimensional column vector of ones,  $\mathbf{W}$  and  $\mathbf{b}$  are the original layer's weight matrix and bias,  $\mathbf{x}$  is the input activation, and  $\oslash$  denotes element-wise division.

A full derivation is provided in Appendix A.6.

Based on this result, the compressed layer is implemented using two linear layers:

• The first layer has weight matrix

$$\mathbf{W}_1 = (\mathbf{U} \odot (\mathbf{a} \cdot \mathbf{1_r}^\top))^\top \mathbf{W}$$

and no bias;

• The second layer has weight matrix

$$\mathbf{W}_2 = \mathbf{U} \oslash (\mathbf{a} \cdot \mathbf{1_r}^\top)$$

and bias

$$\mathbf{b'} = \mathbb{E}[\mathbf{y}] + (\mathbf{U}\mathbf{U}^{\top} \odot (\frac{1}{\mathbf{a}} \cdot \mathbf{a}^{\top}))(\mathbf{b} - \mathbb{E}[\mathbf{y}])$$

The compressed layer is expressed as:

$$\hat{\mathbf{y}} = \mathbf{W}_2(\mathbf{W}_1\mathbf{x}) + \mathbf{b}'$$

# 3.7 IMPACT Algorithm Description

Algorithm 1 outlines the procedure, which consists of two stages: profiling and compression.

#### 3.7.1 Profiling Stage

The algorithm gathers activation and gradient statistics for each linear layer in the model. Specifically, it computes the mean activation, the activation covariance matrix, and the mean squared gradient with respect to the activations. These statistics form the basis for the subsequent compression step.

## 3.7.2 Compression Stage

Using the collected statistics, the algorithm constructs the importance-weighted activation covariance matrix C for each linear layer by applying a Hadamard product between the activation covariance and the gradient-informed importance matrix. Eigenvalue decomposition is then performed on C to extract the top eigenvectors, which define the compression directions. Each original linear layer is subsequently replaced by a pair of smaller linear layers designed to preserve model performance.

# 4 Experiments

# 4.1 Evaluation Methodology

We evaluate the effectiveness of low-rank compression algorithms on two tasks: mathematical reasoning and code generation. For mathematical reasoning, we use the Llama 2-7B and -13B models [Touvron et al., 2023]; for code generation, we use CodeLlama-7B and -13B [Roziere et al., 2023]. Each model is first finetuned on a task-specific finetuning set, then compressed using a low-rank method, and finally undergoes post-compression finetuning before evaluation.

For the mathematical reasoning task, we evaluate on GSM8K [Cobbe et al., 2021] and Hendrycks' MATH [Hendrycks et al., 2021]. For code generation, we use MBPP [Austin et al., 2021] and HumanEval [Chen et al., 2021a] as evaluation sets.

We compare our proposed method, IMPACT, against state-of-the-art low-rank compression techniques, including SVD [Xue et al., 2013, Wang et al., 2021, Noach and Goldberg, 2020, Huang et al., 2021, Li et al., 2023, Lv et al., 2023, Sharma et al., 2024, Lin et al., 2025], a widely used matrix factorization method; FWSVD [Hsu et al., 2022], which incorporates weight importance; and AFM [Yu and Wu, 2023], which performs activation-aware weight matrix compression.

Beyond low-rank methods, we also benchmark IMPACT against compression techniques from other paradigms, including QLoRA [Dettmers et al., 2023], a quantization-based approach that finetunes low-rank adapters, and FLAP [An et al., 2024], a pruning method that removes weights based on magnitude and activation variance. These

#### **Algorithm 1: IMPACT Algorithm**

Input: Model  $\mathcal{L}\mathcal{M}$ 

Output: Compressed Model  $\mathcal{LM}'$  Data: Dataset D, Keeping Ratio k

#### Stage 1: Profiling;

Let n be the total number of samples in D;

**for** each layer l in LM **do** 

Initialize

$$\mathbb{E}[\mathbf{y}\mathbf{y}^{\top}]_{l} = 0, \ \mathbb{E}[\mathbf{y}]_{l} = 0, \ \mathbb{E}[\left(\frac{\partial \ell}{\partial \mathbf{y}}\right)^{2}]_{l} = 0;$$

 $\textbf{for } \textit{each sample } s \in D \textbf{ do}$ 

Get activation  $\mathbf{y}_l$  and gradient  $\frac{\partial \ell}{\partial \mathbf{y}_l}$  for layer l;

for each layer l do

$$\mathbb{E}[\mathbf{y}\mathbf{y}^{\top}]_{l} \leftarrow \mathbb{E}[\mathbf{y}\mathbf{y}^{\top}]_{l} + \mathbf{y}_{l}\mathbf{y}_{l}^{\top};$$

$$\mathbb{E}[\mathbf{y}]_{l} \leftarrow \mathbb{E}[\mathbf{y}]_{l} + \mathbf{y}_{l};$$

$$\mathbb{E}\left[\left(\frac{\partial \ell}{\partial \mathbf{y}}\right)^{2}\right]_{l} \leftarrow \mathbb{E}\left[\left(\frac{\partial \ell}{\partial \mathbf{y}}\right)^{2}\right]_{l} + \left(\frac{\partial \ell}{\partial \mathbf{y}_{l}}\right)^{2};$$

**for** each layer l in **do** 

$$\begin{split} & \mathbb{E} \big[ \mathbf{y} \mathbf{y}^{\top} \big]_{l} \leftarrow \mathbb{E} \big[ \mathbf{y} \mathbf{y}^{\top} \big]_{l} / n; \\ & \mathbb{E} [\mathbf{y}]_{l} \leftarrow \mathbb{E} [\mathbf{y}]_{l} / n; \\ & \mathrm{Cov}(\mathbf{y})_{l} \leftarrow \mathbb{E} [\mathbf{y} \mathbf{y}^{\top}]_{l} - \mathbb{E} [\mathbf{y}]_{l} \, \mathbb{E} [\mathbf{y}]_{l}^{\top}; \end{split}$$

#### **Stage 2: Compression**;

for each layer l do

// For brevity, the subscript l is omitted from the notations presented below.

Compute the transformation coefficient a based on Equation (4);

Compute the gradient-informed importance matrix M based on Equation (12);

Compute the importance-weighted activation covariance matrix C based on Equation (10);

 $[\mathbf{U}, \boldsymbol{\Lambda}] = eigenvalue\_decomposition(\mathbf{C});$ 

// The columns of U are the eigenvectors of C; // The vector  $\Lambda$  consists of the eigenvalues of C;

Sort the elements of  $\Lambda$  in descending order and reorder U accordingly;

Find smallest r such that

$$\left(\sum_{j=1}^r \sqrt{\Lambda_j}\right) / \left(\sum_{j=1}^d \sqrt{\Lambda_j}\right) \ge k/100;$$

 $\mathbf{U} \leftarrow \text{First } r \text{ columns of } \mathbf{U} ;$ 

Substitute the original linear layer with two new linear layers with smaller sizes:

The first new layer has a weight matrix of

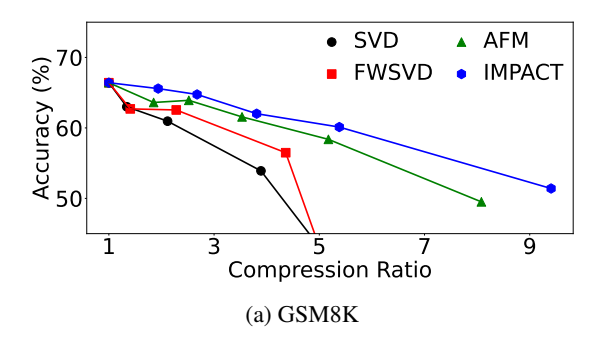
 $(\mathbf{U} \odot (\mathbf{a} \cdot \mathbf{1_r}^\top))^\top \mathbf{W}$  and no bias;

The second new layer has a weight matrix of  $\mathbf{U} \oslash (\mathbf{a} \cdot \mathbf{1_r}^{\top})$  and a bias of

 $\mathbb{E}[\mathbf{y}] + (\mathbf{U}\mathbf{U}^{\top} \odot (\frac{1}{\mathbf{a}} \cdot \mathbf{a}^{\top}))(\mathbf{b} - \mathbb{E}[\mathbf{y}]);$ 

**return** Compressed Model  $\mathcal{LM}'$ ;

comparisons highlight IMPACT's robustness and effectiveness across diverse compression strategies.



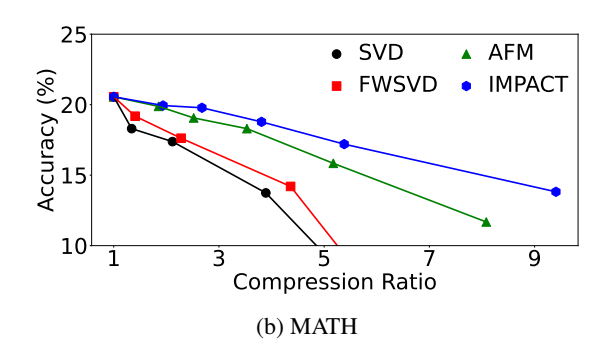
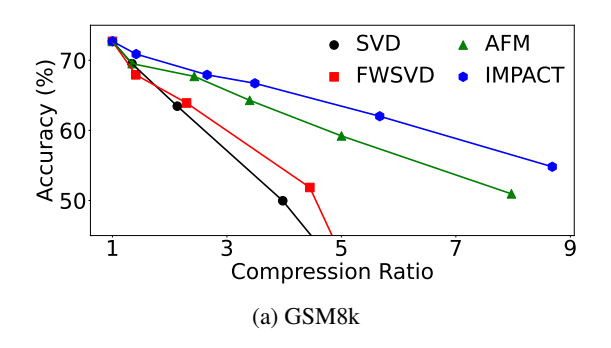


Figure 2: Pass@1 accuracy and model size of Llama 2-7B compressed with various low-rank algorithms on the mathematical reasoning task. Exact values are listed in Table 4 in Appendix B.



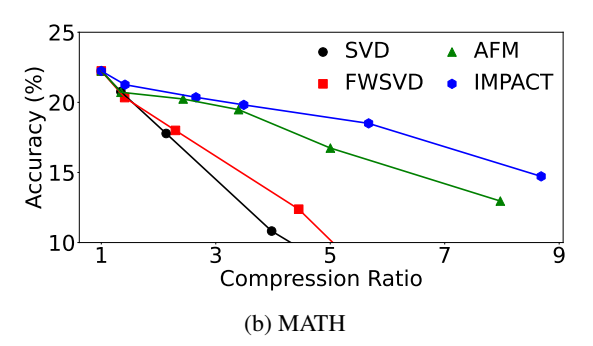


Figure 3: Pass@1 accuracy and model size of Llama 2-13B compressed with various low-rank algorithms on the mathematical reasoning task. Exact values are listed in Table 5 in Appendix B.

# **4.2 Evaluation of Low-Rank Compression 4.3** for Mathematical Reasoning

Figures 2 and 3 show the performance of various low-rank compression methods on Llama2-7B and -13B for the mathematical reasoning task. We evaluate the Pass@1 accuracy of the models across a range of compression ratios (the ratio of the original model size to the compressed model size). Our proposed method, IMPACT, consistently outperforms SVD, FWSVD, and AFM across all compression ratios, achieving greater compression while maintaining comparable or superior accuracy.

On Llama 2-7B, IMPACT achieves up to 48.6% greater size reduction than the best-performing baseline (AFM) on GSM8K, and up to 33.4% more on MATH, while maintaining same accuracy. Across all evaluated compression ratios, it compresses the model over 40% more than SVD and FWSVD on both datasets while delivering similar or better performance. Similar patterns are observed for Llama 2-13B, where IMPACT achieves up to 30.0% more compression than AFM on GSM8K and 32.3% more on MATH. At compression ratios above 2.5×, IMPACT continues to deliver over 40% more compression than SVD and FWSVD on both datasets while maintaining better performance.

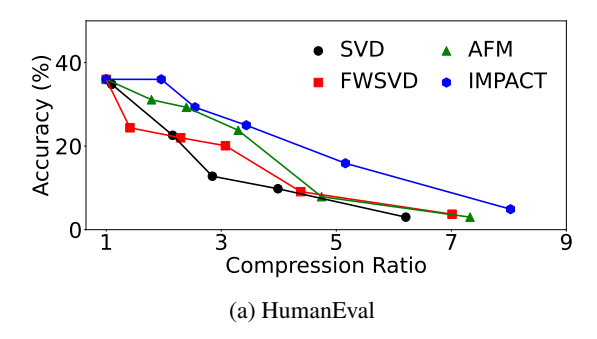
# **4.3 Evaluation of Low-Rank Compression** for Code Generation

Figures 4 and 5 show the performance of IMPACT and baseline compression methods on CodeLlama-7B and -13B for code generation. We evaluate the Pass@1 accuracy on the HumanEval and MBPP benchmarks across a range of compression ratios.

IMPACT consistently outperforms baseline methods by achieving greater compression while maintaining comparable or superior accuracy on both code generation tasks. On CodeLlama-7B, IMPACT reduces model size by up to 48.9% more than the best-performing baseline on HumanEval, and by 14.8% more on MBPP. Similar trends are observed on CodeLlama-13B, where IMPACT achieves up to 28.1% more compression on HumanEval and 15.9% more on MBPP compared to the strongest baseline.

# 4.4 Integrating IMPACT with Quantization

Quantization and low-rank compression are distinct model compression techniques grounded in different principles: quantization reduces the precision of model weights, whereas low-rank compression approximates weight matrices as the product of smaller matrices. Quantization generally preserves performance at 8-bit precision or higher



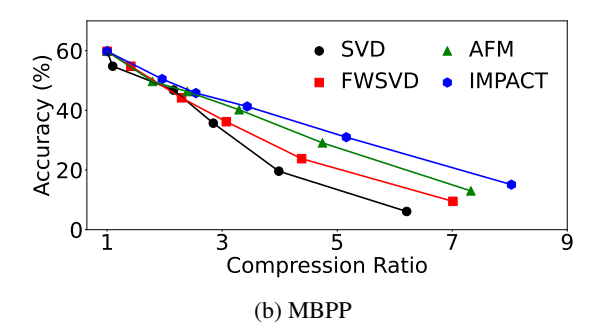
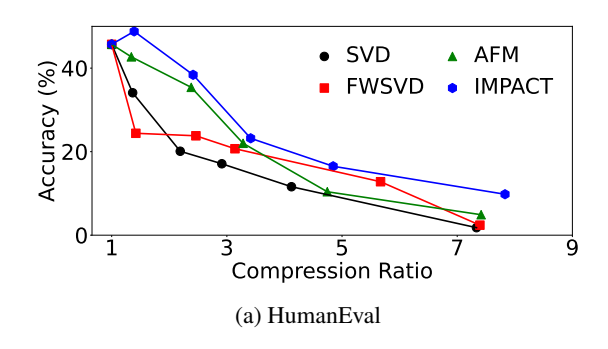


Figure 4: Pass@1 accuracy and model size of CodeLlama-7B compressed with various low-rank algorithms on the code generation task. Exact values are listed in Table 6 in Appendix B.



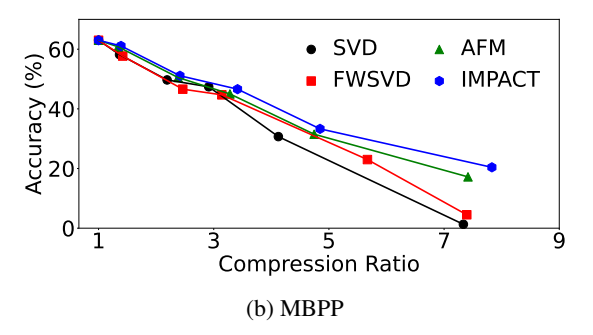


Figure 5: Pass@1 accuracy and model size of CodeLlama-13B compressed with various low-rank algorithms on the code generation task. Exact values are listed in Table 7 in Appendix B.

but often degrades accuracy at lower precisions like 4-bit. To assess the combined effect of quantization and other compression methods such as low-rank compression and pruning, we integrate 8-bit quantization with IMPACT and FLAP to produce compressed models of varying sizes.

Results on the mathematical reasoning task with Llama 2-7B (Figure 6 and Tables 1 and 2) show that IM-PACT with 8-bit quantization consistently outperforms pure 4-bit quantization, 4-bit QLoRA, and 8-bit FLAP. At a comparable model size (3.4 GiB), 8-bit IMPACT yields a 53.86% accuracy improvement over 8-bit FLAP and a 7.16% gain over 4-bit QLoRA on GSM8K. Similar trends are observed for Llama 2-13B (Table 2; Figure 8 and Table 3 in Appendix B), where 8-bit IMPACT again outperforms all baselines. These results highlight both the superior performance of IMPACT and the benefit of combining low-rank compression with quantization, which yields higher accuracy than either technique alone at the same model size.

#### 4.5 Inference Performance

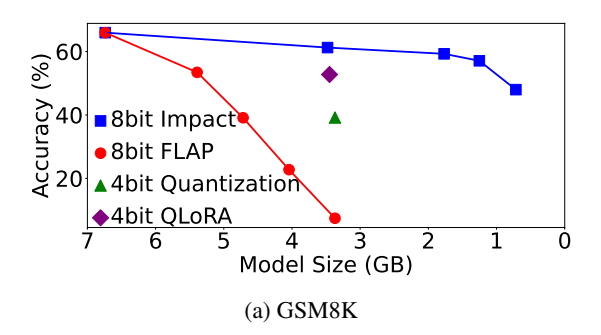
To assess the inference performance of compressed models, we measure their throughput and memory usage on mathematical reasoning tasks. Figure 7 shows the throughput and memory consumption of models compressed with

SVD, FWSVD, AFM, and IMPACT across a range of compression ratios. As expected, larger model sizes result in lower throughput and higher memory usage for all methods. When comparing models of the same size, all approaches exhibit similar throughput and memory consumption. However, because IMPACT achieves comparable accuracy at smaller model sizes than prior methods, it delivers higher throughput and lower memory consumption at the same accuracy level. Specifically, compared to AFM—the strongest baseline—IMPACT improves throughput by up to 35% and reduces memory usage by up to 41%.

# 5 Conclusion

This paper introduces IMPACT, a principled framework for low-rank model compression that explicitly links activation reconstruction to model performance. In contrast to prior methods that either compress weights directly or minimize activation reconstruction error, IMPACT guides activation reconstruction along directions most critical to model behavior. By formulating and solving a well-grounded optimization problem, we derive a closed-form solution in which the optimal reconstruction bases are the eigenvectors of an importance-weighted activation covariance matrix.

Our empirical results across multiple LLMs and mul-



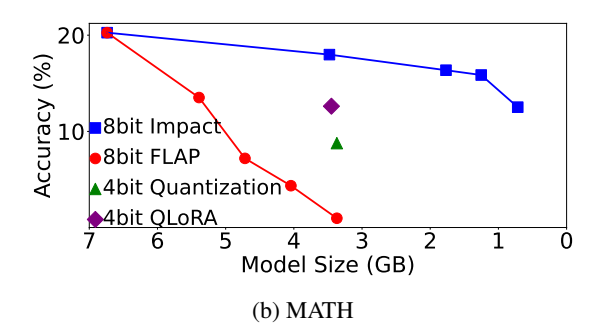


Figure 6: Pass@1 accuracy and model size of Llama 2-7B models compressed using quantization alone, as well as in combination with low-rank compression or pruning techniques, evaluated on the mathematical reasoning task.

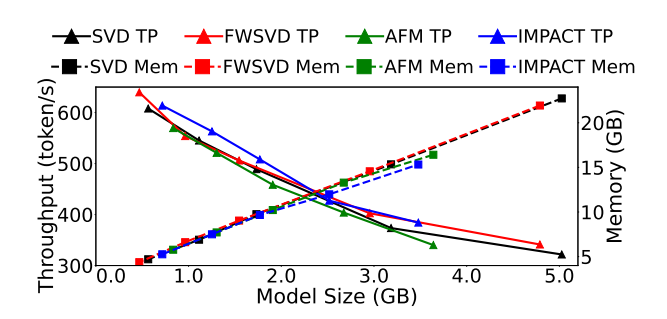


Figure 7: Throughput and memory consumption of compressed models.

Model Variant	Model Size (GB)	Task	Accuracy (%)
4-bit-quantized 7B	3.37	GSM8K MATH	39.2 8.8
4-bit-QLoRA 7B	3.45	GSM8K MATH	54.1 12.6
4-bit-quantized 13B	6.51	GSM8K MATH	52.8 12.5
4-bit-QLoRA 13B	6.63	GSM8K MATH	58.8 13.2

Table 2: Pass@1 accuracy and model size of Llama 2-7B and -13B quantized using standard 4-bit quantization and 4-bit QLoRA on the mathematical reasoning task.

	Model Size (GB)	6.74	5.39	4.72	4.04	3.37
8-bit FLAP	GSM8K Acc (%)	66.0	53.4	39.1	22.7	7.4
	MATH Acc (%)	20.3	13.5	7.2	4.4	1.0
	Model Size (GB)	6.74	3.48	1.77	1.25	0.72
8-bit IMPACT	GSM8K Acc (%)	66.0	61.3	59.3	57.1	48.0
	MATH Acc (%)	20.3	18.0	16.4	15.9	12.5

Table 1: Pass@1 accuracy and model size of 8-bitquantized Llama 2-7B models compressed by FLAP and IMPACT for mathematical reasoning.

tiple benchmarks demonstrate that IMPACT consistently achieves greater compression—up to 48.6% more than prior state-of-the-art—while maintaining similar accuracy. These findings not only validate the theoretical underpinnings of our method but also highlight its practical effectiveness for real-world deployment.

IMPACT offers a general and extensible foundation for future compression research. By establishing a formal link between compression decisions and performance outcomes, our work provides both insight and actionable tools for efficient LLM deployment—advancing the broader goal of making powerful models more accessible and sustainable.

# References

Anish Acharya, Rahul Goel, Angeliki Metallinou, and Inderjit Dhillon. Online Embedding Compression for Text Classification Using Low Rank Matrix Factorization. In Thirty-Third AAAI Conference on Artificial Intelligence and Thirty-First Innovative Applications of Artificial Intelligence Conference and Ninth AAAI Symposium on Educational Advances in Artificial Intelligence, 2019.

Yongqi An, Xu Zhao, Tao Yu, Ming Tang, and Jinqiao Wang. Fluctuation-based Adaptive Structured Pruning for Large Language Models. In *AAAI Conference on Artificial Intelligence*, 2024.

Jacob Austin, Augustus Odena, Maxwell Nye, Maarten Bosma, Henryk Michalewski, David Dohan, Ellen Jiang, Carrie Cai, Michael Terry, Quoc Le, and Charles Sutton. Program Synthesis with Large Language Models. arXiv preprint arXiv:2108.07732, 2021.

Mark Chen, Jerry Tworek, Heewoo Jun, Qiming Yuan, Henrique Ponde de Oliveira Pinto, Jared Kaplan, Harri Edwards, Yuri Burda, Nicholas Joseph, Greg Brockman, et al. Evaluating Large Language Models Trained on Code. *arXiv preprint arXiv:2107.03374*, 2021a.

- Patrick Chen, Si Si, Yang Li, Ciprian Chelba, and Cho-Jui Hsieh. GroupReduce: Block-Wise Low-Rank Approximation for Neural Language Model Shrinking. In Advances in Neural Information Processing Systems (NeurIPS), 2018.
- Patrick Chen, Hsiang-Fu Yu, Inderjit Dhillon, and Cho-Jui Hsieh. DRONE: Data-Aware Low-Rank Compression for Large NLP Models. In *Advances in Neural Information Processing Systems (NeurIPS)*, 2021b.
- Karl Cobbe, Vineet Kosaraju, Mohammad Bavarian, Mark Chen, Heewoo Jun, Lukasz Kaiser, Matthias Plappert, Jerry Tworek, Jacob Hilton, Reiichiro Nakano, Christopher Hesse, and John Schulman. Training Verifiers to Solve Math Word Problems. *arXiv preprint arXiv:2110.14168*, 2021.
- Emily Denton, Wojciech Zaremba, Joan Bruna, Yann Le-Cun, and Rob Fergus. Exploiting linear structure within convolutional networks for efficient evaluation. In *International Conference on Neural Information Processing Systems (NeurIPS)*, 2014.
- Tim Dettmers, Artidoro Pagnoni, Ari Holtzman, and Luke Zettlemoyer. QLoRA: Efficient Finetuning of Quantized LLMs. In *Advances in neural information processing systems (NeurIPS)*, 2023.
- Gene H. Golub and Charles F. Van Loan. *Matrix Computations*. Johns Hopkins University Press, 1983. ISBN 978-0-8018-3010-9.
- Dan Hendrycks, Collin Burns, Saurav Kadavath, Akul Arora, Steven Basart, Eric Tang, Dawn Song, and Jacob Steinhardt. Measuring Mathematical Problem Solving with the MATH Dataset. In *Conference on Neural Information Processing Systems (NeurIPS)*, 2021.
- Yen-Chang Hsu, Ting Hua, Sungen Chang, Qian Lou, Yilin Shen, and Hongxia Jin. Language Model Compression with Weighted Low-Rank Factorization. In *International Conference on Learning Representation (ICLR)*, 2022.
- Shaoyi Huang, Shiyang Chen, Hongwu Peng, Daniel Manu, Zhenglun Kong, Geng Yuan, Lei Yang, Shusen Wang, Hang Liu, and Caiwen Ding. HMC-TRAN: A Tensor-core Inspired Hierarchical Model Compression for Transformer-based DNNs on GPU. In *Great Lakes Symposium on VLSI (GLSVLSI)*, 2021.
- Max Jaderberg, Andrea Vedaldi, and Andrew Zisserman. Speeding up Convolutional Neural Networks with Low Rank Expansions. In *British Machine Vision Conference* (*BMVC*), 2014.

- Yong-Deok Kim, Eunhyeok Park, Sungjoo Yoo, Taelim Choi, Lu Yang, and Dongjun Shin. Compression of Deep Convolutional Neural Networks for Fast and Low Power Mobile Applications. In Yoshua Bengio and Yann LeCun, editors, *International Conference on Learning Representations (ICLR)*, 2016.
- Hailong Li, Jaewan Choi, Yongsuk Kwon, and Jung Ho Ahn. A Hardware-Friendly Tiled Singular-Value Decomposition-Based Matrix Multiplication for Transformer-Based Models. *IEEE Computer Architecture Letters (CAL)*, 22:169–172, 2023.
- Chi-Heng Lin, Shangqian Gao, James Seale Smith, Abhishek Patel, Shikhar Tuli, Yilin Shen, Hongxia Jin, and Yen-Chang Hsu. MoDeGPT: Modular Decomposition for Large Language Model Compression. In *International Conference on Learning Representations (ICLR)*, 2025.
- Zhiyun Lu, Vikas Sindhwani, and Tara N Sainath. Learning Compact Recurrent Neural Networks. In *IEEE International Conference on Acoustics, Speech and Signal Processing (ICASSP)*, 2016.
- Xiuqing Lv, Peng Zhang, Sunzhu Li, Guobing Gan, and Yueheng Sun. LightFormer: Light-weight Transformer Using SVD-based Weight Transfer and Parameter Sharing. In *Findings of the Association for Computational Linguistics (ACL)*, 2023.
- Matan Ben Noach and Yoav Goldberg. Compressing Pretrained Language Models by Matrix Decomposition. In 1st Conference of the Asia-Pacific Chapter of the Association for Computational Linguistics and the 10th International Joint Conference on Natural Language Processing (AACL-IJCNLP), 2020.
- Baptiste Roziere, Jonas Gehring, Fabian Gloeckle, Sten Sootla, Itai Gat, Xiaoqing Ellen Tan, Yossi Adi, Jingyu Liu, Romain Sauvestre, Tal Remez, et al. Code Llama: Open Foundation Models for Code. *arXiv preprint arXiv:2308.12950*, 2023.
- Pratyusha Sharma, Jordan T. Ash, and Dipendra Misra. The Truth is in there: Improving Reasoning in Language Models with Layer-Selective Rank Reduction. In *International Conference on Learning Representations* (*ICLR*), 2024.
- Cheng Tai, Tong Xiao, Yi Zhang, Xiaogang Wang, and E. Weinan. Convolutional Neural Networks With Lowrank Regularization. In *International Conference on Learning Representations (ICLR)*, 2016.
- Hugo Touvron, Louis Martin, Kevin Stone, Peter Albert, Amjad Almahairi, Yasmine Babaei, Nikolay Bashlykov,

Soumya Batra, Prajjwal Bhargava, Shruti Bhosale, et al. Llama 2: Open Foundation and Finetuned Chat Models. *arXiv preprint arXiv:2307.09288*, 2023.

Hongyi Wang, Saurabh Agarwal, and Dimitris Papailiopoulos. Pufferfish: Communication-efficient Models at No Extra Cost. In *Conference on Machine Learning and Systems (MLSys)*, 2021.

Wei Wen, Cong Xu, Chunpeng Wu, Yandan Wang, Yiran Chen, and Hai Li. Coordinating Filters for Faster Deep Neural Networks. In *IEEE International Conference on Computer Vision (ICCV)*, 2017.

Jian Xue, Jinyu Li, and Yifan Gong. Restructuring of Deep Neural Network Acoustic Models with Singular Value Decomposition. In Annual Conference of the International Speech Communication Association (IN-TERSPEECH), January 2013.

Hao Yu and Jianxin Wu. Compressing Transformers: Features Are Low-Rank, But Weights Are Not! In *AAAI Conference on Artificial Intelligence*, 2023.

Zhihang Yuan, Yuzhang Shang, Yue Song, Qiang Wu, Yan Yan, and Guangyu Sun. ASVD: Activation-aware Singular Value Decomposition for Compressing Large Language Models. *arXiv preprint arXiv:2312.05821*, 2023.

Fuzhen Zhang. *The Schur Complement and Its Applications*, volume 4. Springer Science & Business Media, 2006.

# **A** Theoretical Derivation

#### **A.1** Mathematical Preliminaries

To rigorously develop our proposed approach, we first introduce key mathematical definitions and properties that serve as the foundation for our derivation.

**Definition 1** (Differentiation Convention). For a differentiable function  $\ell(\mathbf{y}) : \mathbb{R}^n \to \mathbb{R}$  where  $\mathbf{y} = [y_1, \dots, y_n]^\top \in \mathbb{R}^n$ , the derivative of  $\ell$  with respect to  $\mathbf{y}$  following the denominator-layout convention is given by the row vector

$$\frac{\partial \ell}{\partial \mathbf{y}} = \begin{bmatrix} \frac{\partial \ell}{\partial y_1} & \dots & \frac{\partial \ell}{\partial y_n} \end{bmatrix}$$

We maintain this convention throughout our derivation.

**Definition 2** (Hadamard Product). Given two vectors  $\mathbf{p} = [p_1, \dots, p_n]^{\top} \in \mathbb{R}^n$  and  $\mathbf{q} = [q_1, \dots, q_n]^{\top} \in \mathbb{R}^n$ , the Hadamard product (element-wise product) is defined as

$$\mathbf{p}\odot\mathbf{q}=egin{bmatrix} p_1q_1\ dots\ p_nq_n \end{bmatrix}\in\mathbb{R}^n$$

**Definition 3** (Orthogonality and Normalization). *Given column vectors*  $\mathbf{u_i}, \mathbf{u_j} \in \mathbb{R}^n$ , their orthogonality and normalization properties are defined as follows:

Vectors u<sub>i</sub> and u<sub>j</sub> are orthogonal if their inner product satisfies

$$\mathbf{u_i}^{\mathsf{T}} \mathbf{u_j} = 0$$

 $\bullet$  A vector  $\mathbf{u_i}$  is normalized if

$$\mathbf{u_i}^{\top}\mathbf{u_i} = \left\|\mathbf{u_i}\right\|^2 = 1$$

**Property 1** (QM-AM Inequality). For vector  $\mathbf{y} = [y_1, \dots, y_n]^{\top} \in \mathbb{R}^n$ , the arithmetic mean (AM) and the quadratic mean (QM) are defined as:

$$AM(\mathbf{y}) = \frac{1}{n} \sum_{i=1}^{n} |y_i|, \qquad QM(\mathbf{y}) = \sqrt{\frac{1}{n} \sum_{i=1}^{n} y_i^2}$$

The QM-AM inequality states that: QM  $\geq$  AM if and only if  $|y_1| = \cdots = |y_n|$ .

**Method 1** (Lagrange Multiplier Method). The Lagrange multiplier method determines the local extrema of a function under explicit functional constraints. Given an objective function  $f: \mathbb{R}^n \to \mathbb{R}$  and a constraint function  $g: \mathbb{R}^n \to \mathbb{R}$ , where the constraint is given by g(x) = 0, the Lagrangian function is defined as:

$$\mathcal{L}(x,\lambda) = f(x) + \lambda q(x)$$

where  $\lambda \in \mathbb{R}$  is the Lagrange multiplier. The optimal solution is obtained by solving the system of equations:

$$\frac{d}{dx}\mathcal{L}(x,\lambda) = 0, \quad \frac{d}{d\lambda}\mathcal{L}(x,\lambda) = 0$$

## **A.2** Bounding Theorem

**Theorem 1.** Suppose the loss function  $\ell$  is  $C^1$ -smooth, and the activation dimension is d, the objective function

$$f(\{\mathbf{u}_{\mathbf{k}}\}) = \alpha \mathbb{E}[\|\mathbf{y} - \hat{\mathbf{y}}\|^2] + \beta \mathbb{E}[(\ell(\mathbf{y}) - \ell(\hat{\mathbf{y}}))^2]$$
(14)

is upper bounded by:

$$f(\{\mathbf{u_k}\}) \leq \mathbb{E}\left[\left\|\sqrt{\beta d \mathbb{E}\left[\left(\frac{\partial \ell}{\partial \mathbf{y}}\right)^2\right]^\top + \alpha} \odot (\mathbf{y} - \hat{\mathbf{y}})\right\|^2\right]$$

*Proof.* Performing Taylor expansion on the loss function, we can get:

$$\ell(\hat{\mathbf{y}}) \approx \ell(\mathbf{y}) + \frac{\partial \ell}{\partial \mathbf{y}}(\hat{\mathbf{y}} - \mathbf{y})$$

The higher-order terms (e.g., second order and beyond) are ignored because they are computationally expensive to estimate and difficult to capture accurately in practical applications. Plugging this into Equation (14), we get the following results:

$$f(\{\mathbf{u_k}\}) \approx \alpha \mathbb{E}[\|\mathbf{y} - \hat{\mathbf{y}}\|^2] + \beta \mathbb{E}\left[\left(\frac{\partial \ell}{\partial \mathbf{y}}(\mathbf{y} - \hat{\mathbf{y}})\right)^2\right]$$
$$= \alpha \mathbb{E}[\|\mathbf{y} - \hat{\mathbf{y}}\|^2] + \beta d^2 \mathbb{E}\left[\left(\frac{\frac{\partial \ell}{\partial \mathbf{y}}(\mathbf{y} - \hat{\mathbf{y}})}{d}\right)^2\right]$$
$$\approx \alpha \mathbb{E}[\|\mathbf{y} - \hat{\mathbf{y}}\|^2] + \beta d^2 \left(\frac{\mathbb{E}\left[\frac{\partial \ell}{\partial \mathbf{y}}\right] \mathbb{E}[\mathbf{y} - \hat{\mathbf{y}}]}{d}\right)^2$$

Further based on the QM-AM inequality, we get:

$$f(\{\mathbf{u}_{\mathbf{k}}\}) \le \alpha \mathbb{E}[\|\mathbf{y} - \hat{\mathbf{y}}\|^2] + \beta d\mathbb{E}\left[\left(\frac{\partial \ell}{\partial \mathbf{y}}\right)^2\right] \mathbb{E}[(\mathbf{y} - \hat{\mathbf{y}})^2]$$
(15)

Finally, using the Hadamard product (Definition 2), we get:

$$f(\{\mathbf{u_k}\}) \leq \mathbb{E}\left[\left\|\sqrt{\beta d \,\mathbb{E}\left[\left(\frac{\partial \ell}{\partial \mathbf{y}}\right)^2\right]^\top + \alpha} \odot (\mathbf{y} - \hat{\mathbf{y}})\right\|^2\right]$$

# A.3 Activation Space Transformation Theorem

**Theorem 2.** Applying the projection condition

$$\mathbf{a}\odot(\mathbf{\hat{y}}-\mathbb{E}[\mathbf{y}]) = \left(\sum_k \mathbf{u_k} \mathbf{u_k}^\top\right) \mathbf{a}\odot(\mathbf{y}-\mathbb{E}[\mathbf{y}])$$

where the transformation coefficient a is

$$\mathbf{a} = \sqrt{(1 - \eta) \frac{\mathbb{E}\left[\left(\frac{\partial \ell}{\partial \mathbf{y}}\right)^{2}\right]^{\top}}{\frac{1}{d}\mathbb{E}\left[\left\|\frac{\partial \ell}{\partial \mathbf{y}}\right\|^{2}\right]} + \eta}$$

and utilizing the activation transformation  $\mathbf{\tilde{y}} = \mathbf{a} \odot (\mathbf{y} - \mathbb{E}[\mathbf{y}])$ , the objective

$$h(\{\mathbf{u_k}\}) = \mathbb{E} \Bigg[ \Bigg\| \sqrt{rac{(1-\eta)}{rac{1}{d}\mathbb{E} \left[ \|rac{\partial \ell}{\partial \mathbf{y}} \|^2 
ight]}} \mathbb{E} \left[ \left(rac{\partial \ell}{\partial y}
ight)^2 
ight]^{ op} + \eta \odot (\mathbf{y} - \mathbf{\hat{y}}) \Bigg\|^2 \Bigg]$$

becomes:

$$h(\{\mathbf{u}_{\mathbf{k}}\}) = \mathbb{E}\left[\tilde{\mathbf{y}}^{\top} \left(\mathbf{I} - \sum_{k} \mathbf{u}_{k} \mathbf{u}_{k}^{\top}\right) \tilde{\mathbf{y}}\right]$$
(16)

*Proof.* Using the transformation coefficient **a**, the upper bound function can be written as

$$h(\{\mathbf{u_k}\}) = \mathbb{E}[\|\mathbf{a} \odot (\mathbf{y} - \hat{\mathbf{y}})\|^2]$$
 (17)

Given the projection condition

$$\mathbf{a}\odot\left(\hat{\mathbf{y}}-\mathbb{E}[\mathbf{y}]\right) = \left(\sum_{k}\mathbf{u_{k}}\mathbf{u_{k}}^{\top}\right)\mathbf{a}\odot\left(\mathbf{y}-\mathbb{E}[\mathbf{y}]\right),$$

subtracting  $\mathbf{a} \odot (\mathbf{y} - \mathbb{E}[\mathbf{y}])$  on both sides and, after that, multiplying both sides with -1, we have

$$\mathbf{a} \odot (\mathbf{y} - \hat{\mathbf{y}}) = \left(\mathbf{I} - \sum_{k} \mathbf{u_k} \mathbf{u_k}^{\top}\right) \mathbf{a} \odot (\mathbf{y} - \mathbb{E}[\mathbf{y}])$$
 (18)

Combining Equations (17) and (18), we obtain:

$$h(\{\mathbf{u_k}\}) = \mathbb{E}\left[\left\|\left(\mathbf{I} - \sum_k \mathbf{u_k} \mathbf{u_k}^{\top}\right) \mathbf{a} \odot (\mathbf{y} - \mathbb{E}[\mathbf{y}])\right\|^2\right]$$

Given the transformed activation  $\tilde{\mathbf{y}} = a \odot (\mathbf{y} - \mathbb{E}[\mathbf{y}])$ , the objective function can be rewritten as:

$$\begin{split} h(\{\mathbf{u}_{\mathbf{k}}\}) &= \mathbb{E}\left[\left\|\left(\mathbf{I} - \sum_{k} \mathbf{u}_{k} \mathbf{u}_{k}^{\top}\right) \tilde{\mathbf{y}}\right\|^{2}\right] \\ &= \mathbb{E}\left[\tilde{\mathbf{y}}^{\top} \left(\mathbf{I} - \sum_{k} \mathbf{u}_{k} \mathbf{u}_{k}^{\top}\right) \cdot \left(\mathbf{I} - \sum_{k} \mathbf{u}_{k} \mathbf{u}_{k}^{\top}\right) \tilde{\mathbf{y}}\right] \\ &= \mathbb{E}\left[\tilde{\mathbf{y}}^{\top} \left(\mathbf{I} - 2\sum_{k} \mathbf{u}_{k} \mathbf{u}_{k}^{\top} + \sum_{i,j} \mathbf{u}_{i} \mathbf{u}_{i}^{\top} \mathbf{u}_{j} \mathbf{u}_{j}^{\top}\right) \tilde{\mathbf{y}}\right] \end{split}$$

As  $\{\mathbf{u_k}\}$  are orthogonal vectors where  $\mathbf{u_i u_j}^{\top} = 0$  if  $i \neq j$ , we obtain:

$$h(\{\mathbf{u_k}\}) = \mathbb{E}\left[\tilde{\mathbf{y}}^{\top} \left(\mathbf{I} - 2\sum_{k} \mathbf{u_k} \mathbf{u_k}^{\top} + \sum_{k} \mathbf{u_k} \mathbf{u_k}^{\top}\right) \tilde{\mathbf{y}}\right]$$
$$= \mathbb{E}\left[\tilde{\mathbf{y}}^{\top} \left(\mathbf{I} - \sum_{k} \mathbf{u_k} \mathbf{u_k}^{\top}\right) \tilde{\mathbf{y}}\right]$$

## A.4 Weighted Covariance Matrix

**Theorem 3.** The importance-weighted activation covariance matrix  $\mathbf{C}$ , given by  $\mathbf{C} = \mathbb{E} \big[ \mathbf{\tilde{y}} \mathbf{\tilde{y}}^{\top} \big]$ , is equal to the Hadamard product of the activation covariance matrix  $\mathrm{Cov}(\mathbf{y})$  and the gradient-informed importance matrix  $\mathbf{M}$ , i.e.,

$$\mathbf{C} = \mathrm{Cov}(\mathbf{y}) \odot \mathbf{M}$$

where

$$Cov(\mathbf{y}) = \mathbb{E}\left[ (\mathbf{y} - \mathbb{E}[\mathbf{y}])(\mathbf{y} - \mathbb{E}[\mathbf{y}])^T \right]$$

$$\mathbf{M} = \mathbf{a} \mathbf{a}^{\top}$$

*Proof.* As the importance-weighted activation covariance matrix  $\mathbf{C}$  is given by  $\mathbf{C} = \mathbb{E} \left[ \mathbf{\tilde{y}} \mathbf{\tilde{y}}^{\top} \right]$ , plugging the activation transformation  $\mathbf{\tilde{y}} = \mathbf{a} \odot (\mathbf{y} - \mathbb{E}[\mathbf{y}])$  into this expression matrix  $\mathbf{C}$  can be written as:

$$\begin{aligned} \text{matrix } \mathbf{C} \text{ can be written as:} \\ \mathbf{C} &= \mathbb{E} \left[ (\mathbf{a} \odot (\mathbf{y} - \mathbb{E}[\mathbf{y}])) \left( \mathbf{a} \odot (\mathbf{y} - \mathbb{E}[\mathbf{y}]) \right)^\top \right] \end{aligned}$$

11

The  $(i, j)^{\text{th}}$  element of  $\mathbf{C}$  is:

$$\mathbf{C}_{ij} = \mathbb{E}[\mathbf{a}_i(y_i - \mathbb{E}[y_i]) \cdot a_j(y_j - \mathbb{E}[y_j])]$$

where  $a_i$ ,  $a_j$  and  $y_i$  and  $y_j$  are the  $i^{\text{th}}$  and  $j^{\text{th}}$  elements of a and y, respectively. Since a is a deterministic vector, the expectation becomes:

$$\mathbf{C}_{ij} = a_i a_j \mathbb{E}[(y_i - \mathbb{E}[y_i]) \cdot (y_j - \mathbb{E}[y_j])]$$

The term  $\mathbb{E}[(y_i - \mathbb{E}[y_i]) \cdot (y_j - \mathbb{E}[y_j])]$  is the  $(i, j)^{\text{th}}$  element of the covariance matrix  $\text{Cov}(\mathbf{y})$ , which is given by:

$$\mathrm{Cov}(\mathbf{y}) = \mathbb{E} \Big[ (\mathbf{y} - \mathbb{E}[\mathbf{y}]) (\mathbf{y} - \mathbb{E}[\mathbf{y}])^{\top} \Big]$$

Thus,

$$\mathbf{C}_{ij} = a_i a_j \operatorname{Cov}(\mathbf{y})_{ij}$$

For the gradient-informed importance matrix  $\mathbf{M}$ , which is defined as  $\mathbf{M} = \mathbf{a}\mathbf{a}^{\top}$ , we have  $\mathbf{M}_{ij} = a_i a_j$ . Hence, the  $(i,j)^{\text{th}}$  element of matrix  $\mathbf{C}$  can be expressed as

$$\mathbf{C}_{ij} = \mathbf{M}_{ij} \mathrm{Cov}(\mathbf{y})_{ij}$$

Therefore, the importance-weighted activation covariance matrix C is the Hadamard product of the covariance matrix Cov(y) and the gradient-informed importance matrix M:

$$\mathbf{C} = \operatorname{Cov}(\mathbf{v}) \odot \mathbf{M}$$

**Corollary 1.** The importance-weighted activation covariance matrix **C** is positive semidefinite and symmetric.

*Proof.* The gradient-informed importance matrix  $\mathbf{M}$ , which is given by  $\mathbf{M} = \mathbf{a}\mathbf{a}^{\top}$ , is positive semidefinite and symmetric. Similarly, the covariance matrix  $\mathrm{Cov}(\mathbf{y})$ , which is given by

$$Cov(\mathbf{y}) = \mathbb{E}\left[ (\mathbf{y} - \mathbb{E}[\mathbf{y}])(\mathbf{y} - \mathbb{E}[\mathbf{y}])^{\top} \right],$$

is also positive semidefinite and symmetric. According to the Schur product theorem [Zhang, 2006], the Hadamard product of two positive semidefinite matrices is also positive semidefinite. Therefore, the importance-weighted activation covariance matrix  $\mathbf{C} = \mathbf{M} \odot \mathrm{Cov}(\mathbf{y})$  is positive semidefinite and symmetric.

## A.5 Reconstruction Direction Theorem

**Theorem 4.** To minimize the objective  $h(\{\mathbf{u}_k\})$  under the orthonormal constraints, the optimal  $k^{\mathrm{th}}$  reconstruction direction  $\mathbf{u}_k$  is the eigenvector corresponding to the  $k^{\mathrm{th}}$  largest eigenvalue of the importance-weighted activation covariance matrix  $\mathbf{C}$ .

*Proof.* Taking the partial derivative of the Lagrangian function with respect to each reconstruction direction  $\mathbf{u_k}$  and setting it to zero yields the optimality condition:

$$\frac{\partial L}{\partial \mathbf{u_k}} = -2u_k^{\top} \mathbf{C} + 2\lambda_k \mathbf{u_k}^{\top} = 0$$

Rearranging this equation and taking the transpose of both sides, we obtain:

$$\mathbf{C}^{\top}\mathbf{u}_{\mathbf{k}} = \mathbf{u}_{\mathbf{k}}\lambda_{k}$$

Since the matrix  $\mathbf{C}$  is symmetric (as established in Corollary 1), we can tell  $\mathbf{C} = \mathbf{C}^{\top}$ . By substituting this property, we arrive at:

$$\mathbf{C}\mathbf{u}_{\mathbf{k}} = \lambda_k \mathbf{u}_{\mathbf{k}} \tag{19}$$

From the Equation (16), we get:

$$h(\{\mathbf{u_k}\}) = \mathbb{E}\left[\tilde{\mathbf{y}}^{\top}\tilde{\mathbf{y}}\right] - \mathbb{E}\left[\tilde{\mathbf{y}}^{\top}\sum_{k}\mathbf{u_k}\mathbf{u_k}^{\top}\tilde{\mathbf{y}}\right]$$

$$= \mathbb{E}\left[\tilde{\mathbf{y}}^{\top}\tilde{\mathbf{y}}\right] - \sum_{k}\mathbb{E}\left[\tilde{\mathbf{y}}^{\top}\mathbf{u_k}\mathbf{u_k}^{\top}\tilde{\mathbf{y}}\right]$$

$$= \mathbb{E}\left[\tilde{\mathbf{y}}^{\top}\tilde{\mathbf{y}}\right] - \sum_{k}\mathbb{E}\left[\mathbf{u_k}^{\top}\tilde{\mathbf{y}}\tilde{\mathbf{y}}^{\top}\mathbf{u_k}\right]$$

$$= \mathbb{E}\left[\tilde{\mathbf{y}}^{\top}\tilde{\mathbf{y}}\right] - \sum_{k}\mathbf{u_k}^{\top}\mathbb{E}\left[\tilde{\mathbf{y}}\tilde{\mathbf{y}}^{\top}\right]\mathbf{u_k}$$

As 
$$\mathbf{C} = \mathbb{E}[\tilde{\mathbf{y}}\tilde{\mathbf{y}}^{\top}],$$

$$h(\{\mathbf{u_k}\}) = \mathbb{E}\left[\tilde{\mathbf{y}}^{\top}\tilde{\mathbf{y}}\right] - \sum_{k} \mathbf{u_k}^{\top} \mathbf{C} \mathbf{u_k}$$

Further based on Equation (19),

$$h(\{\mathbf{u}_{\mathbf{k}}\}) = \mathbb{E}\left[\tilde{\mathbf{y}}^{\top}\tilde{\mathbf{y}}\right] - \sum_{k} \mathbf{u_{k}}^{\top} \mathbf{u_{k}} \lambda_{k}$$
$$= \mathbb{E}\left[\tilde{\mathbf{y}}^{\top}\tilde{\mathbf{y}}\right] - \sum_{k} \|\mathbf{u_{k}}\|^{2} \lambda_{k}$$

 $As \|\mathbf{u_k}\|^2 = 1,$ 

$$h(\{\mathbf{u_k}\}) = \mathbb{E}\Big[\mathbf{\tilde{y}}^{\top}\mathbf{\tilde{y}}\Big] - \sum_k \lambda_k$$

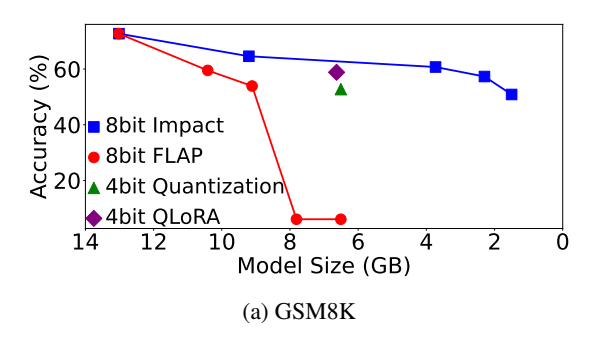
To minimize  $h(\{\mathbf{u_k}\})$ , the term  $\sum_k \lambda_k$  must be maximized. Since the importance-weighted activation covariance matrix  $\mathbf{C}$  is symmetric and positive semidefinite, its eigenvalues are real and non-negative. Therefore, the maximum value of  $\sum_k \lambda_k$  is achieved when  $\lambda_k$  is the  $k^{\mathrm{th}}$  largest eigenvalues of  $\mathbf{C}$ , with  $\mathbf{u_k}$  its corresponding eigenvector.

# **A.6** Activation Reconstruction Theorem

**Theorem 5.** The reconstructed activation  $\hat{\mathbf{y}}$ , which satisfies the projection condition

$$\mathbf{a}\odot\left(\mathbf{\hat{y}}-\mathbb{E}[\mathbf{y}]
ight) = \left(\sum_{k}\mathbf{u_{k}}\mathbf{u_{k}}^{ op}
ight)\mathbf{a}\odot\left(\mathbf{y}-\mathbb{E}[\mathbf{y}]
ight),$$

is given by:



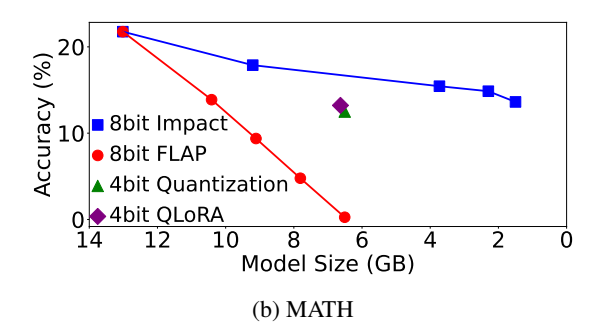


Figure 8: Pass@1 accuracy and model size of Llama 2-13B models compressed using quantization alone, as well as in combination with low-rank compression or pruning techniques, evaluated on the mathematical reasoning task. Tables 2 and 3 present the exact values.

	Model Size (GB)	13.02	10.41	9.11	7.81	6.51
8-bit FLAP	GSM8K Acc (%)	72.7	59.5	53.9	6.1	6.1
	MATH Acc (%)	21.8	13.9	9.4	4.8	0.3
	Model Size (GB)	13.02	9.21	3.73	2.30	1.50
8-bit IMPACT	GSM8K Acc (%)	72.7	64.6	60.7	57.3	50.9
	MATH Acc (%)	21.8	17.9	15.4	14.9	13.6

Table 3: Pass@1 accuracy and model size of 8-bit-quantized Llama 2-13B models compressed by FLAP and IMPACT for mathematical reasoning.

$$\begin{split} \hat{\mathbf{y}} &= \left[\mathbf{U} \oslash (\mathbf{a} \cdot \mathbf{1_r}^\top)\right] \left[ (\mathbf{U} \odot (\mathbf{a} \cdot \mathbf{1_r}^\top))^\top \mathbf{W} \right] \mathbf{x} \\ &+ (\mathbf{U} \oslash (\mathbf{a} \cdot \mathbf{1_r}^\top)) (\mathbf{U} \odot (\mathbf{a} \cdot \mathbf{1_r}^\top))^\top (\mathbf{b} - \mathbb{E}[\mathbf{y}]) + \mathbb{E}[\mathbf{y}] \end{split}$$

where  $\mathbf{U} = [\mathbf{u}_1, \dots, \mathbf{u}_r]$ ,  $\mathbf{1}_r$  is an r-dimensional column vector of ones,  $\mathbf{W}$  and  $\mathbf{b}$  are the original layer's weight matrix and bias,  $\mathbf{x}$  is the input activation, and  $\odot$  denotes element-wise (Hadamard) division.

Proof. Rearranging the projection condition

$$\mathbf{a}\odot\left(\mathbf{\hat{y}}-\mathbb{E}[\mathbf{y}]
ight) = \left(\sum_{k}\mathbf{u_{k}}\mathbf{u_{k}}^{ op}
ight)\mathbf{a}\odot\left(\mathbf{y}-\mathbb{E}[\mathbf{y}]
ight),$$

we obtain

$$\mathbf{a} \odot (\mathbf{\hat{y}} - \mathbb{E}[\mathbf{y}]) = \sum_k \mathbf{u_k} (\mathbf{u_k} \odot \mathbf{a})^\top (\mathbf{y} - \mathbb{E}[\mathbf{y}]))$$

Applying the Hadamard division  $\oslash \mathbf{a}$  to both sides of the equation leads to:

$$\mathbf{\hat{y}} - \mathbb{E}[\mathbf{y}] = \sum_{k} \mathbf{u_k} (\mathbf{u_k} \odot \mathbf{a})^{ op} (\mathbf{y} - \mathbb{E}[\mathbf{y}]) \oslash \mathbf{a}$$

Since  $(\mathbf{u_k} \odot \mathbf{a})^{\top}$  is a row vector and  $(\mathbf{y} - \mathbb{E}[\mathbf{y}])$  is a column vector,  $(\mathbf{u_k} \odot a)^{\top} (\mathbf{y} - \mathbb{E}[\mathbf{y}])$  is a scalar, we have

$$\mathbf{\hat{y}} = \mathbb{E}[\mathbf{y}] + \sum_{k} (\mathbf{u_k} \oslash a) (\mathbf{u_k} \odot a)^T (\mathbf{y} - \mathbb{E}[\mathbf{y}])$$

Rewriting the equality, we obtain:

$$\mathbf{\hat{y}} = \mathbb{E}[\mathbf{y}] + (\mathbf{U} \oslash (\mathbf{a} \cdot \mathbf{1_r}^\top)) (\mathbf{U} \odot (\mathbf{a} \cdot \mathbf{1_r}^\top))^\top (\mathbf{y} - \mathbb{E}[\mathbf{y}])$$

where  $\mathbf{U} = [\mathbf{u}_1, \dots, \mathbf{u}_r]$ .

Incorporating the original activation y = Wx + b, we obtain:

$$\mathbf{\hat{y}} = \mathbb{E}[\mathbf{y}] + (\mathbf{U} \oslash (\mathbf{a} \cdot \mathbf{1}_r^\top)) (\mathbf{U} \odot (\mathbf{a} \cdot \mathbf{1}_r^\top))^\top (\mathbf{W} \mathbf{x} + \mathbf{b} - \mathbb{E}[\mathbf{y}])$$

Expanding the expression, the reconstructed activation satisfies:

$$\begin{split} \mathbf{\hat{y}} &= \left[\mathbf{U} \oslash (\mathbf{a} \cdot \mathbf{1_r}^\top)\right] \left[ (\mathbf{U} \odot (\mathbf{a} \cdot \mathbf{1_r}^\top))^\top \mathbf{W} \right] \mathbf{x} \\ &+ (\mathbf{U} \oslash (\mathbf{a} \cdot \mathbf{1_r}^\top)) (\mathbf{U} \odot (\mathbf{a} \cdot \mathbf{1_r}^\top))^\top (\mathbf{b} - \mathbb{E}[\mathbf{y}]) + \mathbb{E}[\mathbf{y}] \end{split}$$

### **B** Additional Results

<sup>&</sup>lt;sup>1</sup>The best baseline refers to the smallest model among SVD, FWSVD, and AFM that achieves accuracy matched to IMPACT. If no baseline exactly matches the accuracy, the model size is interpolated linearly between two adjacent compression points.

	Model Size (Billion)	6.74	5.03	3.18	1.73	1.11	0.56	
SVD	GSM8K Acc (%) MATH Acc (%)	66.4 20.6	63.0 18.3	61.0 17.4	53.9 13.7	32.9 5.3	11.9 2.8	
	Model Size (Billion)	6.74	4.79	2.95	1.54	0.96	0.47	
FWSVD	GSM8K Acc (%) MATH Acc (%)	66.4 20.6	62.7 19.2	62.5 17.6	56.5 14.2	1.5 1.8	1.9 1.5	
	Model Size (Billion)	6.74	3.64	2.67	1.91	1.30	0.83	
AFM	GSM8K Acc (%) MATH Acc (%)	66.4 20.6	63.6 19.9	63.9 19.1	61.6 18.3	58.4 15.8	49.5 11.7	
	Model Size (Billion)	6.74	3.48	2.52	1.77	1.25	0.72	
IMPACT	GSM8K Acc (%) MATH Acc (%)	66.4 20.6	65.6 19.9	64.7 19.8	62.0 18.8	60.1 17.2	51.4 13.8	

(a) Model size and accuracy. The first data point for each method	i
corresponds to the full, uncompressed model.	

GSM8K							
Best Baseline <sup>1</sup> (with Same Acc.)	Model Size (Billion)	5.82	4.90	2.06	1.63	0.93	
IMPACT	Model Size (Billion)	3.48	2.52	1.77	1.25	0.72	
	Size Reduction (%)	40.2	48.6	14.0	23.4	23.3	
	MATH						
Best Baseline <sup>1</sup> (with Same Acc.)	Model Size (Billion)	3.91	3.52	2.39	1.64	1.07	
IMPACT	Model Size (Billion)	3.48	2.52	1.77	1.25	0.72	
	Size Reduction (%)	11.1	28.5	26.0	23.5	33.4	

(b) Size reduction of IMPACT over the best baseline at matched accuracy.

Table 4: Pass@1 accuracy and model size of Llama 2-7B compressed by various algorithms for the mathematical reasoning task.

	Model Size (Billion)	13.02	9.70	6.10	3.27	2.07	1.01
SVD	GSM8K Acc (%)	72.7	69.5	63.5	50.0	26.9	6.7
	MATH Acc (%)	22.2	20.8	17.8	10.8	5.2	2.2
	Model Size (Billion)	13.02	9.24	5.67	2.93	1.79	0.83
FWSVD	GSM8K Acc (%)	72.7	67.9	63.9	51.9	2.4	3.9
	MATH Acc (%)	22.2	20.3	18.0	12.4	1.2	1.9
	Model Size (Billion)	13.02	9.69	5.36	3.83	2.60	1.63
AFM	GSM8K Acc (%)	72.7	69.5	67.7	64.3	59.2	50.9
	MATH Acc (%)	22.2	20.7	20.2	19.5	16.7	13.0
IMPACT	Model Size (Billion)	13.02	9.21	4.90	3.73	2.30	1.50
	GSM8K Acc (%)	72.7	70.9	67.9	66.7	62.0	54.8
	MATH Acc (%)	22.2	21.3	20.4	19.8	18.5	14.7

(a) Model size and accuracy. The first data point for each method corresponds to the full, uncompressed model.

GSM8K							
Best Baseline <sup>1</sup> (with Same Acc.)	Model Size (Billion)	11.11	5.90	4.92	3.28	2.09	
IMPACT	Model Size (Billion)	9.21	4.90	3.73	2.30	1.50	
	Size Reduction (%)	17.2	16.8	24.1	30.0	28.2	
	MATH	I					
Best Baseline <sup>1</sup> Model Size (Billion) 10.82 6.44 4.51 3.39 2.08 (with Same Acc.)				2.08			
IMPACT	Model Size (Billion)	9.21	4.90	3.73	2.30	1.50	
	Size Reduction (%)	14.9	23.8	17.4	32.3	28.1	

(b) Size reduction of IMPACT over the best baseline at matched accuracy.

Table 5: Pass@1 accuracy and model size of Llama 2-13B compressed by various algorithms for the mathematical reasoning task.

	Model Size (Billion)	6.74	6.14	3.13	2.37	1.69	1.09
SVD	HumanEval Acc (%)	36.0	34.8	22.6	12.8	9.8	3.0
	MBPP Acc (%)	59.8	54.8	46.8	35.7	19.6	6.1
	Model Size (Billion)	6.74	4.77	2.94	2.19	1.54	0.96
FWSVD	HumanEval Acc (%)	36.0	24.4	22.0	20.1	9.1	3.7
	MBPP Acc (%)	59.8	54.8	44.2	36.2	23.8	9.5
	Model Size (Billion)	6.74	3.77	2.81	2.05	1.42	0.92
AFM	HumanEval Acc (%)	36.0	31.1	29.3	23.8	7.9	3.0
	MBPP Acc (%)	59.8	49.7	46.3	40.2	29.1	13.0
	Model Size (Billion)	6.74	3.44	2.65	1.96	1.31	0.84
IMPACT	HumanEval Acc (%)	36.0	36.0	29.3	25.0	15.9	4.9
	MBPP Acc (%)	59.8	50.5	45.8	41.3	31.0	15.1

(a) Model size and accuracy. The first data point for each method (a) Model size and accuracy. The first data point for each method corresponds to the full, uncompressed model.

HumanEval								
Best Baseline <sup>1</sup> (with Same Acc.)	Model Size (Billion)	6.74	2.81	2.21	1.73	1.09		
IMPACT	Model Size (Billion)	3.44	2.65	1.96	1.31	0.84		
IVII / ICT	Size Reduction (%)	48.9	5.9	11.4	24.7	22.9		
	MBPP							
Best Baseline <sup>1</sup> (with Same Acc.)	Model Size (Billion)	4.00	2.75	2.18	1.53	0.99		
IMPACT	Model Size (Billion)	3.44	2.65	1.96	1.31	0.84		
	Size Reduction (%)	14.0	3.7	10.2	14.5	14.8		

(b) Size reduction of IMPACT over the best baseline at matched accuracy.

Table 6: Pass@1 accuracy and model size of CodeLlama-7B compressed by various algorithms for the code generation task.

	Model Size (Billion)	13.02	9.54	5.94	4.47	3.16	1.77
SVD	HumanEval Acc (%)	45.7	34.1	20.1	17.1	11.6	1.8
	MBPP Acc (%)	63.0	58.2	49.7	47.4	30.7	1.3
	Model Size (Billion)	13.02	9.17	5.29	4.14	2.30	1.76
FWSVD	HumanEval Acc (%)	45.7	24.4	23.8	20.7	12.8	2.4
	MBPP Acc (%)	63.0	57.7	46.6	44.7	23.0	4.5
	Model Size (Billion)	13.02	9.71	5.47	3.97	2.74	1.76
AFM	HumanEval Acc (%)	45.7	42.7	35.4	22.0	10.4	4.9
	MBPP Acc (%)	63.0	60.8	50.5	45.0	31.5	17.2
	Model Size (Billion)	13.02	9.36	5.39	3.81	2.69	1.66
IMPACT	HumanEval Acc (%)	45.7	48.8	38.4	23.2	16.5	9.8
	MBPP Acc (%)	63.0	61.1	51.1	46.6	33.3	20.4

corresponds to the full, uncompressed model.

HumanE	val				
Model Size (Billion)	13.02	7.21	4.10	3.16	2.14
Model Size (Billion)	9.36	5.39	3.81	2.69	1.66
Size Reduction (%)	28.1	25.2	7.0	15.0	22.4
MBPF	)				
Best Baseline <sup>1</sup> Model Size (Billion) 10.16 5.71 4.40 2.91 1.98 (with Same Acc.)					
Model Size (Billion)	9.36	5.39	3.81	2.69	1.66
Size Reduction (%)	7.8	5.6	13.4	7.6	15.9
	Model Size (Billion)  Model Size (Billion)  Size Reduction (%)  MBPF  Model Size (Billion)  Model Size (Billion)	Model Size (Billion)       9.36         Size Reduction (%)       28.1         MBPP         Model Size (Billion)       10.16         Model Size (Billion)       9.36	Model Size (Billion)         13.02         7.21           Model Size (Billion)         9.36         5.39           Size Reduction (%)         28.1         25.2           MBPP           Model Size (Billion)         10.16         5.71           Model Size (Billion)         9.36         5.39	Model Size (Billion)         13.02         7.21         4.10           Model Size (Billion)         9.36         5.39         3.81           Size Reduction (%)         28.1         25.2         7.0           MBPP           Model Size (Billion)         10.16         5.71         4.40           Model Size (Billion)         9.36         5.39         3.81	Model Size (Billion)         13.02         7.21         4.10         3.16           Model Size (Billion)         9.36         5.39         3.81         2.69           Size Reduction (%)         28.1         25.2         7.0         15.0           MBPP           Model Size (Billion)         10.16         5.71         4.40         2.91           Model Size (Billion)         9.36         5.39         3.81         2.69

(b) Size reduction of IMPACT over the best baseline at matched accuracy.

Table 7: Pass@1 accuracy and model size of CodeLlama-13B compressed by various algorithms for the code generation task.